Thoracic Cancer ISSN 1759-7706

ORIGINAL ARTICLE

Diagnosis of the invasiveness of lung adenocarcinoma manifesting as ground glass opacities on high-resolution computed tomography

Haixia Mao, Kanchan Labh, Fushi Han, Sen Jiang, Yang Yang & Xiwen Sun

Department of Radiology, Shanghai Pulmonary Hospital, Tongji University School of Medicine, Shanghai, China

Keywords
Lung neoplasms; neoplasm invasion; tomography; X-ray computed.

Correspondence
Xiwen Sun, Department of Radiology, Shanghai Pulmonary Hospital, Tongji University School of Medicine, 507 Zhengmin Road, Shanghai, 200433, China.
Tel: +86 13816593938
Fax: +86 021 65115006 3089
Email: xiwensunfeike@126.com

Received: 2 March 2015;
Accepted: 29 March 2015.

doi: 10.1111/1759-7714.12269

Thoracic Cancer **7** (2016) 129–135

Abstract

Background: To explore the diagnostic method in assessing the malignancy of pulmonary adenocarcinoma characterized by ground glass opacities (GGO) on computed tomography (CT).

Methods: Preoperative CT data for preinvasive and invasive lung adenocarcinomas were analyzed retrospectively. GGO lesions that were detected on lung windows but absent using the mediastinal window were subject to adjustment of the window width, which was reduced with the fixed interval of 100 HU until the lesions were no longer evident, with a fixed mediastinal window level of 40 HU. The shape, smoking habits, size of the lesion on the lung window, and window width at which lesions disappeared were compared and receiver operating characteristic curves were used to determine the optimal cut-off of the lesion size and window width to differentiate between these invasive and preinvasive lesions.

Results: Of the 209 lung adenocarcinomas, 102 were preinvasive (25 atypical adenomatous hyperplasia and 77 adenocarcinoma in situ), while 107 were invasive (78 minimally invasive adenocarcinoma and 29 invasive adenocarcinoma). The shape, lesion size, and window width at which lesions were no longer evident differed significantly between the two groups ($P < 0.05$). The size of 8.9 mm and a window width of 1250 HU were the optimal cut-off to differentiate between preinvasive and invasive lesions.

Conclusion: The shape, size of the lesion, and window width on high-resolution CT may be useful in assessing the invasiveness of lung adenocarcinoma that manifests as GGO. Irregular lesions that disappear at window width <1250 HU, with a diameter of > 8.9 mm are more likely to be invasive.

Introduction

A ground glass opacity (GGO) is defined using high-resolution computed tomography (HRCT) imaging as a pulmonary shadow comprised of hazy increased attenuation with preservation of the bronchial and vascular margins. Only the solid component of a GGO is evident using the mediastinal window.[1] Although the etiology of a GGO is varied, pulmonary malignancy must be considered and adenocarcinoma is the most common histologic type.[2] The International Association for the Study of Lung Cancer/American Thoracic Society/European Respiratory Society (IASLC/ATS/ERS) proposed a new classification for lung adenocarcinoma which divided lung adenocarcinoma into two main groups: preinvasive lesions, including atypical adenomatous hyperplasia (AAH) and adenocarcinoma in situ (AIS); and invasive lesions, such as minimally invasive adenocarcinoma (MIA), invasive adenocarcinoma, and variants of invasive adenocarcinoma.[3]

Early lung adenocarcinoma detected on HRCT often manifests as GGOs. Many studies have assessed the relationship between radiographic and pathologic data in lung adenocarcinoma, evaluating lesion prognosis by changes in the size of a lesion between the lung and mediastinal windows.[4–6] However, the invasiveness of GGOs, which are visible on lung windows but not on mediastinal windows, cannot be judged by changes in size between these two windows. Clinically, we observed that the apparent size of the tumor can be adjusted with a changing window width and this has led us to study the impact of window width in predicting the invasiveness of lung adenocarcinoma.

Materials and methods

Ethics

The study was performed in accordance with the Declaration of Helsinki and was approved by the ethical committees of Shanghai Pulmonary Hospital and the Tongji University School of Medicine. All participants provided written informed consent.

Clinical cases

The CT images and correlated clinical data of 209 patients with lung adenocarcinoma who attended our hospital from January 2013 to May 2014 were retrospectively collected. Criteria for inclusion into the study included the presence of a GGO with a diameter of less than 2 cm on lung windows but not evident using mediastinal windows, and all cases were diagnosed with lung adenocarcinoma by pathology after surgical treatment. The range of the duration between CT scan and surgical diagnosis was 1–25 days and the mean duration was 5.3 ± 4.3 days. Of the 102 cases of preinvasive lesions, 25 were classed as AAH and 77 were AIS. Of the 107 invasive lesions, 78 were MIA and 29 were invasive adenocarcinoma. Sixty-nine patients were men, and 140 were women; the average age was 55.01 ± 10.48 years; and the average lesion size was 0.94 ± 0.39 cm.

Methods

In all patients included in the study, a thin-section CT was performed preoperatively at least once. In all individuals, thin-section CTs were performed using a Sensation-64 scanner (Siemens, Munich, Germany) with 120 kVp, automatic mAs, bone reconstruction algorithm, a pitch of 1.2, scan field of view of 350 mm, matrix of 512 × 512, and collimation of 128*0.6 mm. Images were reconstructed with 1 mm thickness. For the lung window, the width was 1500 HU, and the level was –450 HU. For the mediastinal window, the width was 400 HU and the level was 40 HU. All images were taken without the use of contrast medium. All CT images were reviewed independently by three senior radiologists with specialist experience in diagnostic imaging on a three million pixel resolution medical display with a fixed mediastinal window level and adjustable mediastinal window width. Vessels within the GGO should be excluded from the regions of interest and the highest density part should be included. Multiplanar reconstruction was performed when necessary. Results were calculated as the average of the report findings of the three independent radiologists who were unaware of the pathological diagnosis. Where necessary, discrepancies were resolved by team review involving all three radiologists.

Statistical methods

All data were processed using SPSS 20.0 statistical software (IBM Corp., Armonk, NY, USA). The Pearson χ^2 test was used for comparison of the lesion shape and patient's smoking habits between preinvasive and invasive lesions. The sample mean of the lesion size on lung window and the window width at which lesions were no longer evident between preinvasive and invasive lesions was tested (if the sample followed normal distribution and homogeneity of variance, a *t*-test was used, otherwise, a nonparametric rank sum test was used), and receiver operating characteristic (ROC) curves were drawn according to the results. The area under the curve (AUC), sensitivity, and specificity were obtained using various cut-off points and the optimal cut-off point was defined as that having the greatest AUC. Measurement data were written in $x \pm$ s. The difference was considered statistically significant if $P < 0.05$.

Results

Of 209 cases of lung adenocarcinoma, 102 cases were preinvasive and 107 were invasive lesions. The basic characteristics of these lesions are shown in Table 1. The size of the lesion on the lung window and window width at which preinvasive and invasive lesions were no longer evident did not conform to normal ($P < 0.05$, Table 2). The Pearson χ^2 and nonparametric rank sum test were performed and showed that the shape, size of lesion, and window width at which lesions were no longer apparent differed between preinvasive and invasive lesions ($P < 0.05$, Table 3). The ROC curves showed that lesion size and window width were good indicators for the invasiveness of pulmonary adenocarcinoma ($P < 0.05$), with a size of 8.9 mm and a width of 1250 HU being the optimal the cut-off for differentiating between invasive and noninvasive lesions (Table 4). Lesions that disappeared with a window

Table 1 The basic characteristics of preinvasive and invasive lesions

	Preinvasive lesions	Invasive lesions	Total
Gender			
Male	36	33	69
Female	66	74	140
Mean age (years)	53.61 ± 10.75	56.36 ± 10.08	55.01 ± 10.48
Number of lesions			
Solitary	52	62	114
Multiple	50	45	95

Table 2 Shapiro-Wilk test for the normality of size and window width

	Statistics	Degrees of freedom	*P*
Size			
Preinvasive lesions	0.914	102	0
Invasive lesions	0.915	107	0
Window width			
Preinvasive lesions	0.948	102	0.001
Invasive lesions	0.956	107	0.001

width >1250 HU and a size of < 8.9 mm were more likely to be preinvasive, while those that disappeared with a window width <1250 HU and size of > 8.9 mm were more likely to be invasive lesions (Figs 1, 2).

Discussion

The relationship between the new classification of lung adenocarcinoma proposed by IASLC/ATS/ERS and the CT features of GGO, which were visible on lung windows but invisible on mediastinal windows, was investigated. We have demonstrated that the size of the tumor as adjusted by the change of the window width can assist in the differential diagnosis of preinvasive and invasive lesions. We measured the size of the lesion on the lung window and window width at which lesions were no longer evident in the context of a fixed mediastinal window level of 40 HU, and subjected our results to the nonparametric rank sum test. A Pearson χ^2 test was used to compare the shape and smoking habits. The results demonstrated that shape, lesion size, and window width at which lesions were no longer evident differed significantly between the two groups ($P < 0.05$). From the resulting ROC curves, lesion size and window width were found to be good predictors for the diagnosis of the invasiveness and, therefore, the prognosis of the tumor ($P < 0.05$). The AUC was the largest at a size of 8.9 mm and window width of 1250 HU. Irregular lesions that had a size of >8.9 mm and disappeared

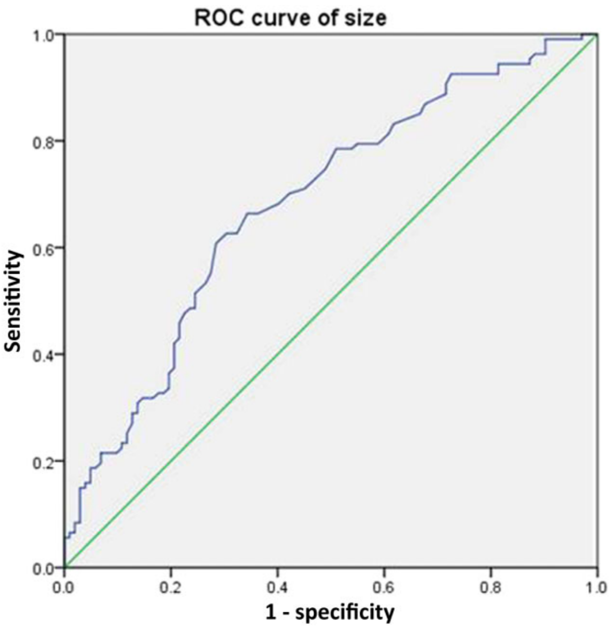

Figure 1 Receiver operating characteristic (ROC) curve analysis, size

Table 3 The comparision between preinvasive and invasive lesions

	Preinvasive lesions	Invasive lesions	Statistics	*P*
Shape*				
Round	99	92	8.142	0.004
Irregular	3	15		
Smoking habits*				
Smoker	24	27	0.082	0.774
Non-smoker	78	80		
Lesion size (mm)†	8.3 ± 2.9	1.04 ± 3.7	–4.571	0.000
Window width†	1306.5 ± 188.8	1085.0 ± 188.8	–6.297	0.000

*Pearson χ^2 test. † Nonparametric rank sum test.

Table 4 Area under the ROC curve of lesion size and window width

			95% confidence interval		
	Area	*P*	Lower limit	Upper limit	Optimal cut-off
Lesion size	0.683	0.000	0.611	0.755	8.9 mm (sensitivity = 0.607, specificity = 0.716)
Window width	0.749	0.000	0.682	0.816	1250 HU (sensitivity = 0.578, specificity = 0.850)

ROC, receiver operating characteristic.

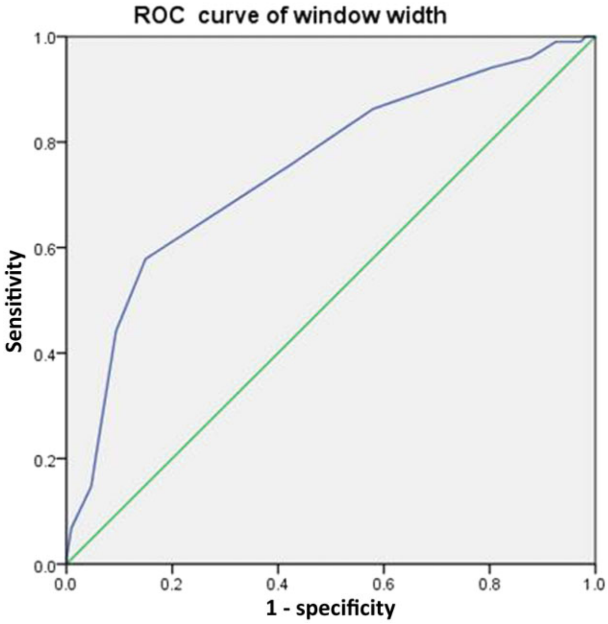

Figure 2 Receiver operating characteristic (ROC) curve analysis, width.

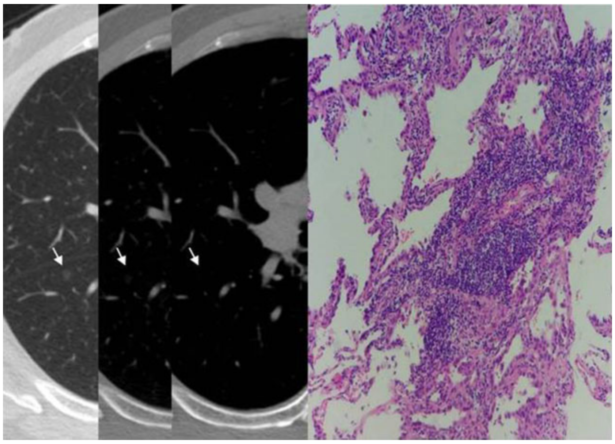

Figure 3 A 63 year-old male patient with a pathological diagnosis of atypical adenomatous hyperplasia (hematoxylin-eosin stain, ×200). The computed tomography image shows a 4 mm ground glass opacity in the right lower lobe. From left to right, followed by lung window, mediastinal window width of 1800 HU, 1600 HU, and 1500 HU. The size of the lesion decreased gradually and was invisible at a mediastinal window width of 1500 HU.

at a window width of >1250 HU were more likely to be preinvasive compared with those that disappeared at <1250 HU.

The window level is the center gray level in the image displayed on CT. It is this level that the CT attenuation of the structures being observed should be set, to permit the proper evaluation of structural detail. Window width can affect the contrast of the image. Many researchers have investigated the relationship between window settings and the form of nodules, and have determined that the adjustment of the window width and window level can highlight tissue boundaries, and individualized window widths and levels can provide more precise detail.[7,8] In this study, we investigated the relationship between the window width at which lesions were no longer apparent and the invasiveness and prognosis of lung adenocarcinoma, and found that window settings could assist in the differential diagnosis of subtypes of lung adenocarcinoma. Window width is the range of CT value shown on CT images; the range of CT value decreases with the decrease of window width, which can explain the difference between visibility of preinvasive and invasive lesions. In our study, the imaging was observed with a fixed mediastinal window level of 40 HU, and the component that had a low CT value disappeared when the window width decreased with a fixed interval of 100 HU and the component of lesion that could be visible decreased. Tsutani *et al*. found that the solid component was related to the malignance of lung adenocarcinoma.[9] The choice of window settings is an important consideration when CT is used to assess the size of pulmonary nodules: previous studies have variously reported that tumor prognosis may be estimated by the size of the tumor, or that tumor size did not correlate with disease stage or prognosis in lung tumors of size <30 mm.[10,11] In our clinical experience, the size of a tumor will be adjusted with the change of the window width. Moreover, the adjustment of window width required to cause lesions to become invisible varied between different types of lung adenocarcinoma (Figs 3–6). Management of the different types of lung adenocarcinomas varies, in part because of their different prognoses; therefore, it is

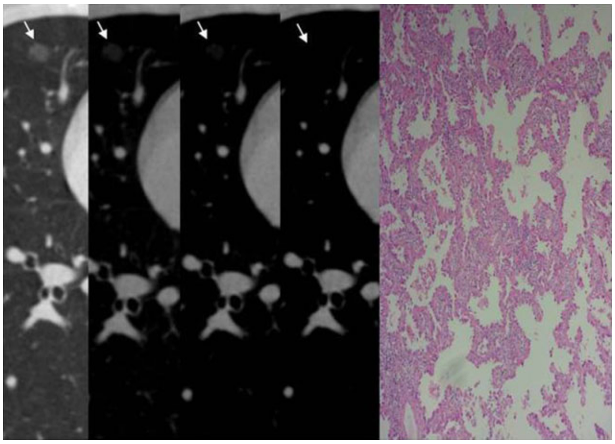

Figure 4 A 39 year-old female patient with a pathological diagnosis of adenocarcinoma in situ (hematoxylin-eosin stain, ×100). The computed tomography image shows a 6 mm ground glass opacity in the right middle lobe. From left to right, followed by lung window, mediastinal window width of 1800 HU, 1600 HU, 1400 HU, and 1300 HU. The size of the lesion decreased gradually and was invisible on the mediastinal window with a window width of 1300 HU.

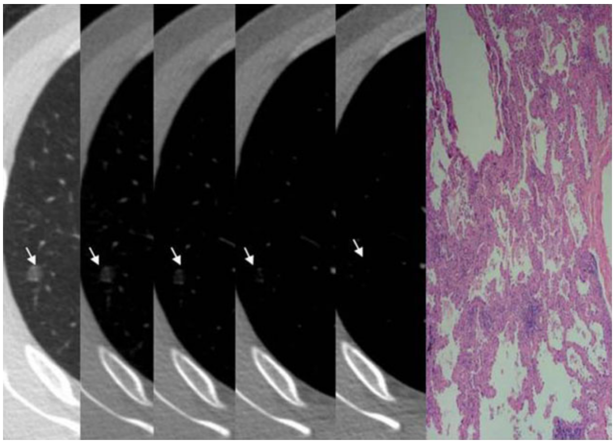

Figure 5 A 57 year-old male patient with a pathological diagnosis of minimally invasive adenocarcinoma (hematoxylin-eosin stain, ×100). In the right upper lobe there was a 6.5 mm ground glass opacity on computed tomography. From left to right, followed by lung window, mediastinal window width of 1800 HU, 1600 HU, 1400 HU, 1200 HU, and 1000 HU. The size of the lesion decreased gradually and was invisible with a mediastinal window width of 1000 HU.

critical to form an accurate judgment of the invasiveness and prognosis of the tumor preoperatively.[12,13] Previous studies have found that the size of the tumor, the size of the solid tumor component, the extent of pathologic invasion, and the GGO ratio are important predictors of prognosis.[14–18] The length, area, modified length, and vanishing ratio method for predicting five-year relapse-free survival have been evaluated using ROC analysis, with the vanishing ratio method being found to be the most accurate predictor.[19] Tumors have also been classified into air-containing and solid-density type according to the attenuation of the tumor opacity between the lung and mediastinal windows, with the air-containing type having a better prognosis than solid-density type adenocarcinomas.[20] However, this method is not suitable for assessing the invasiveness and prognosis of GGOs that are only visible on lung windows.

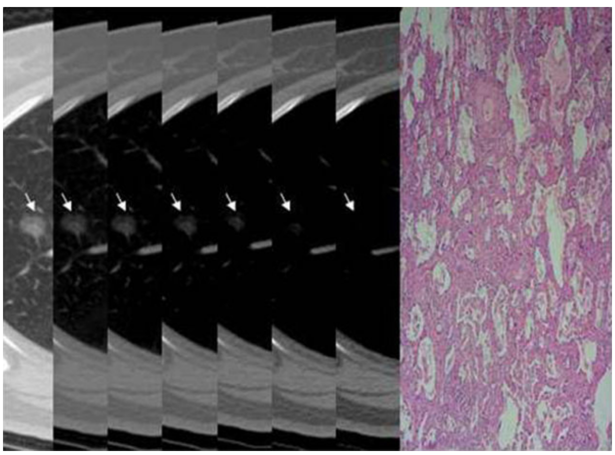

Figure 6 A 55 year-old male patient with a pathological diagnosis of invasive adenocarcinoma (hematoxylin-eosin stain, ×100). The computed tomography image shows a 12-mm ground glass opacity in the right upper lobe. From left to right, followed by lung window, mediastinal window width of 1800 HU, 1600 HU, 1400 HU, 1200 HU, 1000 HU, and 900 HU. The size of the lesion decreased gradually and was invisible at a mediastinal window width of 900 HU.

Atypical adenomatous hyperplasia and AIS gradually develop into invasive adenocarcinomas in a dynamic process that is thought to involve the accumulation of mutations in several genes.[21,22] The new classification of lung adenocarcinoma proposed by IASLC/ATS/ERS classifies lung adenocarcinoma into preinvasive and invasive lesions. Relevant scholars have suggested that comparing the CT value of different subtypes could lead to a diagnosis of lung adenocarcinoma.[23,24] The CT value and the adjustment of window width methods changed according to the different densities of different subtypes of lung adenocarcinoma, with the CT value easily affected by partial volume effect.

In addition, we found that an irregular lesion with a maximum diameter of >8.9 mm was helpful to distinguish between preinvasive and invasive lesions. Jin *et al*. suggested that the optimal cut-off value for discriminating preinvasive from MIA was 8.17 mm, which is consistent with our findings.[25] A GGO that disappeared at a window width of <1250 HU with an irregular shape, in addition to a diameter of > 8.9 mm, was more likely to be an invasive adenocarcinoma.

This study aimed to predict the presence of an invasive component in lung adenocarcinoma by observing the window width at which lesions were no longer visible. The method chosen in the present study was reproducible and simple, and would be suitable for providing guidance for preoperative diagnosis. However, there were several limitations to our study. First, the finding of early lung adenocarcinoma on HRCT was centrilobular GGO in the context of vessel involvement, yet vessels within the GGO should be excluded from the regions of interest. Second, we were unable to extend our findings to an analysis of the specific differences between enhanced and routine scans. The reasons the differences in lesion window width were no longer evident between invasive and preinvasive lesions may be attributed to variation in scanning parameters between different instruments, the resolution of the display, or simple observer error.

Conclusions

The results of our study have significance for clinical practice, permitting a more rational radiologic approach to the specific pathological subtypes of lung adenocarcinoma through the manipulation of window widths. We anticipate that further prospective study and the generation of more precise software will extend our observations.

Acknowledgment

We would like to acknowledge the reviewers for their helpful comments on this paper.

Disclosure

No authors report any conflict of interest.

References

1 Kitami A, Kamio Y, Hayashi S *et al*. One-dimensional mean computed tomography value evaluation of ground-glass opacity on high-resolution images. *Gen Thorac Cardiovasc Surg* 2012; **60**: 425–30.

2 Stringer BK, Cooper AG, Shepard SB. Overexpression of the G-protein inwardly rectifying potassium channel 1 (GIRK1) in primary breast carcinomas correlates with axillary lymph node metastasis. *Cancer Res* 2001; **61**: 582–8.

3 Travis WD, Brambilla E, Noguchi M *et al*. International Association for the Study of Lung Cancer/American Thoracic Society/European Respiratory Society international multidisciplinary classification of lung adenocarcinoma. *J Thorac Oncol* 2011; **6**: 244–85.

4 Kondo T, Yamada K, Noda K, Nakayama H, Kameda Y. Radiologic-prognostic correlation in patients with small pulmonary adenocarcinomas. *Lung Cancer* 2002; **36**: 49–57.

5 Ikehara M, Saito H, Yamada K *et al*. Prognosis of small adenocarcinoma of the lung based on thin-section computed tomography and pathological preparations. *J Comput Assist Tomogr* 2008; **32**: 426–31.

6 Ikehara M, Saito H, Kondo T *et al*. Comparison of thin-section CT and pathological findings in small solid-density type pulmonary adenocarcinoma: Prognostic factors from CT findings. *Eur J Radiol* 2012; **81**: 189–94.

7 Mehta SB, Chaudhury S, Bhattacharyya A, Jena A. A soft-segmentation visualization scheme for magnetic resonance images. *Magn Reson Imaging* 2005; **23**: 817–28.

8 Fuji H, Asada Y, Numano M *et al*. Residual motion and duty time in respiratory gating radiotherapy using individualized or population-based windows. *Int J Radiat Oncol Biol Phys* 2009; **75**: 564–70.

9 Tsutani Y, Miyata Y, Nakayama H *et al*. Prognostic significance of using solid versus whole tumor size on high-resolution computed tomography for predicting pathologic malignant grade of tumors in clinical stage IA lung adenocarcinoma: A multicenter study. *J Thorac Cardiovasc Surg* 2012; **143**: 607–12.

10 Yang F, Chen H, Xiang J *et al*. Relationship between tumor size and disease stage in non-small cell lung cancer. *BMC Cancer* 2010; **10**: 474.

11 Patz EF Jr, Rossi S, Harpole DH Jr, Herndon JE, Goodman PC. Correlation of tumor size and survival in patients with stage IA non-small cell lung cancer. *Chest* 2000; **117**: 1568–71.

12 Haro A, Yano T, Kohno M, Yoshida T, Okamoto T, Maehara Y. Ground-glass opacity lesions on computed tomography during postoperative surveillance for primary non-small cell lung cancer. *Lung Cancer* 2012; **76**: 56–60.

13 Murakawa T, Konoeda C, Ito T *et al*. The ground glass opacity component can be eliminated from the T-factor assessment of lung adenocarcinoma. *Eur J Cardiothorac Surg* 2013; **43**: 925–32.

14 Morgensztern D, Waqar S, Subramanian J, Gao F, Trinkaus K, Govinden R. Prognostic significance of tumor size in patients with stage III non-small-cell lung cancer: A surveillance, epidemiology, and end results (SEER) survey from 1998 to 2003. *J Thorac Oncol* 2012; **7**: 1479–84.

15 Maeyashiki T, Suzuki K, Hattori A, Matsunaga T, Takamochi K, Oh S. The size of consolidation on thin-section computed tomography is a better predictor of survival than the maximum tumour dimension in resectable lung cancer. *Eur J Cardiothorac Surg* 2013; **43**: 915–8.

16 Tsutani Y, Miyata Y, Mimae T *et al*. The prognostic role of pathologic invasive component size, excluding lepidic growth, in stage I lung adenocarcinoma. *J Thorac Cardiovasc Surg* 2013; **146**: 580–5.

17 Uehara H, Tsutani Y, Okumura S *et al*. Prognostic role of positron emission tomography and high-resolution computed tomography in clinical stage IA lung adenocarcinoma. *Ann Thorac Surg* 2013; **96**: 1958–65.

18 Okada M, Nakayama H, Okumura S *et al*. Multicenter analysis of high-resolution computed tomography and positron emission tomography/computed tomography findings to choose therapeutic strategies for clinical stage IA lung adenocarcinoma. *J Thorac Cardiovasc Surg* 2011; **141**: 1384–91.

19 Kakinuma R, Kodama K, Yamada K *et al*. Performance evaluation of 4 measuring methods of ground-glass opacities for predicting the 5-year relapse-free survival of patients with peripheral nonsmall cell lung cancer: A multicenter study. *J Comput Assist Tomogr* 2008; **32**: 792–8.

20 Honda T, Kondo T, Murakami S *et al*. Radiographic and pathological analysis of small lung adenocarcinoma using the new IASLC classification. *Clin Radiol* 2013; **68**: e21–6.

21 Lee HJ, Goo JM, Lee CH, Yoo CG, Kim YT, Im JG. Nodular ground-glass opacities on thin-section CT: Size change during follow-up and pathological results. *Korean J Radiol* 2007; **8**: 22–31.

22 Min JH, Lee HY, Lee KS *et al*. Stepwise evolution from a focal pure pulmonary ground-glass opacity nodule into an invasive lung adenocarcinoma: An observation for more than 10 years. *Lung Cancer* 2010; **69**: 123–6.

23 Ikeda K, Awai K, Mori T, Kawanaka K, Yamashita Y, Nomori H. Differential diagnosis of ground-glass opacity nodules: CT number analysis by three-dimensional computerized quantification. *Chest* 2007; **132**: 984–90.

24 Nomori H, Ohtsuka T, Naruke T, Suemasu K. Differentiating between atypical adenomatous hyperplasia and bronchioloalveolar carcinoma using the computed tomography number histogram. *Ann Thorac Surg* 2003; **76**: 867–71.

25 Ge X, Gao F, Li M *et al*. [Diagnostic value of solid component for lung adenocarcinoma shown as ground-glass nodule on computed tomography.] *Zhonghua Yi Xue Za Zhi* 2014; **94**: 1010–3. (In Chinese.)